


Received: 28 November 2023 | Accepted: 11 June 2024

DOI: 10.1002/jcp.31343

RESEARCH ARTICLE

Journal of Cellular Physiology WILEY

RhoB plays a central role in hyperosmolarity-induced cell shrinkage in renal cells

Mariangela Centrone¹ | Ilaria Saltarella² | Mariagrazia D'Agostino¹ |
Marianna Ranieri¹ | Maria Venneri³ | Annarita Di Mise¹ | Laura Simone⁴ |
Francesco Pisani¹ | Giovanna Valenti¹ | Maria A. Frassanito⁵ | Grazia Tamma¹ 

¹Department of Biosciences Biotechnologies and Environment, University of Bari Aldo Moro, Bari, Italy

²Department of Precision and Regenerative Medicine and Ionian Area, Section of Pharmacology, School of Medicine, University of Bari Aldo Moro, Bari, Italy

³Istituti Clinici Scientifici Maugeri SPA SB IRCCS, Bari, Italy

⁴Fondazione IRCCS Casa Sollievo della Sofferenza, Cancer Stem Cells Unit, San Giovanni Rotondo, Italy

⁵Department of Precision and Regenerative Medicine and Ionian Area, Section of Clinical Pathology, University of Bari Aldo Moro, Bari, Italy

Correspondence

Grazia Tamma, Department of Bioscience, Biotechnology and Environment, University of Bari Aldo Moro, Via Orabona 4, Bari 70125, Italy.
Email: grazia.tamma@uniba.it

Funding information

Ministero dell'Università e della Ricerca

Abstract

The small Rho GTP-binding proteins are important cell morphology, function, and apoptosis regulators. Unlike other Rho proteins, RhoB can be subjected to either geranylgeranylation (RhoB-GG) or farnesylation (RhoB-F), making that the only target of the farnesyltransferase inhibitor (FTI). Fluorescence resonance energy transfer experiments revealed that RhoB is activated by hyperosmolarity. By contrast, hyposmolarity did not affect RhoB activity. Interestingly, treatment with farnesyltransferase inhibitor-277 (FTI-277) decreased the cell size. To evaluate whether RhoB plays a role in volume reduction, renal collecting duct MCD4 cells and Human Kidney, HK-2 were transiently transfected with RhoB-wildtype-Enhance Green Fluorescence Protein (RhoB-wt-EGFP) and RhoB-CLLL-EGFP which cannot undergo farnesylation. A calcein-based fluorescent assay revealed that hyperosmolarity caused a significant reduction of cell volume in mock and RhoB-wt-EGFP-expressing cells. By contrast, cells treated with FTI-277 or expressing the RhoB-CLLL-EGFP mutant did not properly respond to hyperosmolarity with respect to mock and RhoB-wt-EGFP expressing cells. These findings were further confirmed by 3D-LSCM showing that RhoB-CLLL-EGFP cells displayed a significant reduction in cell size compared to cells expressing RhoB-wt-EGFP. Moreover, flow cytometry analysis revealed that RhoB-CLLL-EGFP expressing cells as well as FTI-277-treated cells showed a significant increase in cell apoptosis. Together, these data suggested that: (i) RhoB is sensitive to hyperosmolarity and not to hyposmolarity; (ii) inhibition of RhoB farnesylation associates with an increase in cell apoptosis, likely suggesting that RhoB might be a paramount player controlling apoptosis by interfering with responses to cell volume change.

KEYWORDS

cell volume, hyperosmolarity, kidney, RhoB, Rho GTP-binding proteins

1 | INTRODUCTION

A crucial feature of animal cells is their capability to control and modulate their cell volume. Even though mammalian cells live in a highly controlled external environment, they can face extracellular and intracellular osmotic changes. This is particularly true for renal cells that have to tackle either rapid alterations of osmolality or prolonged periods dealing with very high external osmolarity. Importantly, changes in renal urinary concentration and excretion depend on the levels of salt load and body hydration. Therefore, increased levels of NaCl and urea may lead to inner medulla (IM) hyperosmolality. However, the relative contribution of these osmoles is different due to their differential cell permeability. Indeed, NaCl does not easily enter the cells thus leading to hypertonicity. In this respect, hypertonic NaCl can cause DNA double-strand breaks, oxidative stress, and thus protein carbonylation which is a common feature observed in several renal diseases including diabetic nephropathy and chronic kidney disease (Kültz, 2004). In addition, the application of osmotic agents, used as antiadhesive materials, can lead to acute kidney injury (Economidou et al., 2011). Notably, cell volume regulation is a crucial process associated with a number of physiological events including receptor recycling, hormone release, cell death, and growth, proliferation, and migration (Okada et al., 2001; Sardini et al., 2003). Physiologically, cells can swell or shrink in response to osmotic perturbation. Over a wide range of external osmolality, a linear correlation between changes in external osmotic pressure and variation in cell volume has been described (Venkova et al., 2022). Indeed, as a consequence of an osmotic shock, a first passive response, due to water flux, occurs at a timescale of seconds. Also, changes in the cell volume are related to the state of actin cortex polymerization and membrane tension coupled to ion transport (Venkova et al., 2022). Both hypo-osmotic and hyperosmotic stress cause deep actin remodeling involving several actin-binding and actin-regulator proteins including the Rho-GTPases. Hypotonicity causes a significant loss of actin stress fibers and the formation of F-actin patches at the cell border possibly in a calcium-dependent manner. These changes are associated with the activation of Rac and Cdc42 (Carton et al., 2003; Erickson et al., 2003; Tamma, Procino, Strafino, et al., 2007; Tamma, Procino, Svelto, et al., 2007). In renal collecting duct CD8 cells, hypotonicity caused the recruitment of the ezrin-moesin-radixin (ERM) protein moesin at the membrane protrusion (Tamma, Procino, Svelto, et al., 2007). The ERM proteins can crosslink the membrane to the underlying cortical actin cytoskeleton playing therefore a role in modulating membrane tension (Liu et al., 2012). On the other hand, hyperosmotic stress activates ERM proteins and phosphorylation independently of the Rho-kinase pathway (Rasmussen et al., 2008). Nevertheless, in renal cells (LLC-PK1 and Madin-Darby canine kidney) hyperosmotic stress causes a significant increase in F-actin content through the Rho/ROCK/LIMK-mediated signal pathway (Thirone et al., 2009). The Rho-GTPases are involved in controlling cell morphology mostly by modulating actin cytoskeleton dynamics. RhoA, RhoB, and RhoC constitute a subfamily within the Rho-GTPases family. These

monomeric G-proteins share a high degree of homology and function (Vega & Ridley, 2018). However, RhoB differs from RhoA and RhoC as it can be not only geranylgeranylated but also farnesylated (Vega & Ridley, 2018). These post-translational modifications play a role in regulating the functions and cellular localization of RhoB (Prendergast, 2001b). Treatment with farnesyltransferase inhibitors (FTIs) alters the ratio between the farnesylated respect to the geranylgeranylated (F:GG) form of RhoB, as in the presence of a specific FTI, only RhoB-GG can be synthesized (Prendergast, 2001a). In vitro studies revealed that RhoB-GG is mainly located in the multivesicular late endosomes whereas RhoB-F is localized at the plasma membrane (Wherlock et al., 2004). Besides controlling cell migration, morphology, and polymerization of the actin cytoskeleton, RhoB displays selective and pleiotropic roles including mammalian development, inflammation, DNA damage responses, intracellular trafficking, and signaling (Liu et al., 2001; Pan & Yeung, 2005; Vega & Ridley, 2018). Interestingly, a number of studies report that RhoB can act as a tumor suppressor due to different lipid modifications (Ju & Gilkes, 2018). Specifically, selective inhibition of farnesylation, by using FTIs, increases the abundance of the geranylgeranylated form of RhoB that reduces cell proliferation and promotes FTIs-dependent apoptosis (Du & Prendergast, 1999). Apoptosis is a programmed form of cell death involving several cleaving enzymes and is characterized by DNA fragmentation, bleb formations, and cell shrinkage even under physiological normotonic conditions (Chaouhan et al., 2022; Maeno et al., 2000). Physiologically, hyperosmolarity leads to cell shrinkage even though adaptive strategies, including cytoskeletal reorganization, take place to blunt the adverse effects associated with the hyperosmotic shock. Nevertheless, extensive cell shrinkage can be considered harmful to cell integrity and function; moreover, prolonged or intense hyperosmolar stress also triggers apoptosis (Yue & López, 2020). In this respect, it has been proposed that specific external osmotic conditions may also reduce cancer cell growth (Svetlitsyna et al., 2024). In human neutrophils, hypertonicity causes a robust and sustained activation of Rac and Cdc42 which might be responsible for actin remodeling (Lewis et al., 2002). Rac1 and Cdc42 can also play a role in inducing cell apoptosis (Arrazola Sastre et al., 2020). However, the mechanism and the protein players involved in hypertonicity and apoptosis remain still elusive. In the present study, the cellular responses to hyperosmolarity on RhoB function were investigated in renal cells. Specifically, we found that RhoB is selectively activated by hyperosmolarity and not by hyposmolarity. Also, the inhibition of RhoB farnesylation is associated with a significant cell size decrease, apoptosis, and an abnormal response to hyperosmolarity in terms of shrinkage.

2 | MATERIALS AND METHODS

2.1 | Cell culture

Mouse Cortical Collecting Duct cells (MCD4) (Iolascon et al., 2007) were grown in Dulbecco's modified Eagle's medium (DMEM/F12)

supplemented with 5% (v/v) fetal bovine serum (FBS), 1% (v/v) L-glutamine, 100 IU/mL penicillin, 100 µg/mL streptomycin, 5 µM dexamethasone. The human kidney proximal tubular epithelial HK-2 cells were maintained in DMEM Ham's F12 medium supplemented with 10% FBS, 100 IU/ml penicillin, 100 µg/mL streptomycin, and 0.01% epidermal growth factor (EGF), 1% (v/v) L-glutamine at 37°C in 5% CO₂. Routinely cells were tested for Mycoplasma with MycoSPY[®] Master Mix (DUOTECH SRL) or by fluorescence staining with DAPI. The cells were maintained at 37°C in a 5% CO₂ incubator.

2.2 | Plasmids

The intramolecular RhoB FRET sensor was kindly obtained by Professor Jaap van Buul (Reinhard et al., 2016). RhoB-wildtype-Enhance Green Fluorescence Protein (EGFP-RhoB-wt) and EGFP-RhoB-CLLL were kindly gifted by Professor Staffan Strömblad (Gong et al., 2018).

2.3 | Transfection

MCD4 cells were transfected as previously described (Centrone et al., 2022). Briefly, cells were grown on 12 mm diameter glass coverslips and transiently transfected with plasmids (with 0.5 µg of DNA) encoding for the RhoB FRET sensor. Alternatively, cells were transfected with RhoB-wt-EGFP or its variant RhoB-CLLL-EGFP, using TransFectin[™] Lipid Reagent (1.5 µL) according to the protocol provided by the manufacturer (Bio-Rad Laboratories Inc.). HK-2 cells were transfected with plasmids (0.5 µg of DNA) encoding for EGFP-RhoB-wt and EGFP-RhoB-CLLL, using Lipofectamine[™] 2000 (0.77 µL) according to the protocol provided by the manufacturer (Life Technologies). All experiments were performed 48 h after transfection.

2.4 | Fluorescence Resonance Energy Transfer (FRET) measurements

To evaluate RhoB activity, FRET experiments were performed as already described (Henn et al., 2004). Briefly, cells were seeded onto 25 mm diameter glass coverslips and transiently transfected with a plasmid encoding for the RhoB FRET sensor (3 µg of DNA), using TransFectin[™] Lipid Reagent (9 µL). The intramolecular FRET sensor has been already described by Reinhard et al. (2016). Cells were left under isotonic solutions obtained with sodium chloride (iso-NaCl) or mannitol (iso-M) (0.5 mM MgCl₂, 2.7 mM KCl, 1 mM CaCl₂, 10 mM HEPES, pH7.4 supplemented with 145 mM NaCl or 245 mM Mannitol, 300 mOsm/L). After recording the fluorescence signal under isotonic conditions, cells were exposed to hypertonic sodium chloride (hyper-NaCl) or mannitol (hyper-M) solution gradients (400 and 500 mOsm/L). Solution osmolarities were measured using a vapor pressure osmometer (Wescor). Detection of FRET was

performed on an inverted microscope (Nikon Eclipse TE2000-S) controlled by Metafluor[®] Software (Molecular Devices, MDS Analytical Technologies).

2.5 | Cell volume measurements

Cells were grown onto a six multiwell plate and were left under basal condition or treated with 10 µM farnesyltransferase inhibitor-277 (FTI-277) for 48 h. Cultured cells were detached with trypsin and centrifuge at 1500 rpm for 5 min. Then, the pellet was resuspended in 1 mL of isotonic sodium chloride (NaCl) or mannitol (M) solution for 5 min at room temperature. Cell size was measured by electronic cell sizing (LUNA-II[™] Automated Cell Counter).

Cell volume was also measured using a calcein-quenching method. Briefly, permeabilized calcein-AM is metabolized to fluorescence calcein in the cells. Calcein fluorescence can be quenched by protein in a concentration-dependent manner. However, on short timescales considering the intracellular protein concentration being constant, calcein fluorescence could be used as a probe of cell volume (Kitchen et al., 2020). Here, cells were seeded onto 25 mm diameter glass coverslips and were left under basal conditions or stimulated with 10 µM FTI-277 for 48 h. Cells were loaded with 10 µM membranes permeable calcein green-AM for 45 min at 37°C, 5% CO₂ in DMEM, and exposed to isotonic NaCl or M solutions. Alternatively, cells were transfected with GFP-tagged proteins and loaded with 10 µM calcein red-orange (Thermo Fisher Scientific). The coverslips with dye-loaded cells were mounted in a perfusion chamber (FCS2 Closed Chamber System, BIOPTCHS) and single-cell measurements were performed using an inverted fluorescence microscope (Nikon ECLIPSE TE2000-S) equipped with a cooled CCD camera controlled by the Metamorph Microscopy Automation and Image Analysis Software (Molecular Devices LLC). Calcein green fluorescence was excited at 490 nm and detected at 520 nm, whereas calcein red-orange fluorescence was excited at 577 nm and detected at 590 nm. Cells in iso-NaCl or iso-M solution were exposed to hyper-NaCl or hyper-M solution gradient (400 and 500 mOsm/L) for 2 min. To normalize the intracellular fluorescence levels within cells, recorded average fluorescence signals were ratioed to the total area of each cell since calcein fluorescence, on a short timescale, changes proportionally to changes in cell size (Kitchen et al., 2020).

2.6 | Confocal microscopy, 3D-reconstruction, and measurement of cell volume using Z-stacks confocal images

MCD4 and HK-2 cells were grown on 12 mm diameter glass coverslips and transfected with GFP-tagged proteins as mentioned before. At 80% confluence, cells were fixed in 4% paraformaldehyde solution for 20 min and washed with PBS. Cells were mounted onto glass slides with Mounting medium (50% glycerol in 0.2 M Tris-HCl, pH 8.0, containing 2.5% n-propyl gallate).

Confocal microscopy was performed using a Leica TCS SP5 microscope. XYZ-series were acquired with a raster size of 1024 × 1024 px in the X–Y planes and a Z-step of 0.2 μm between optical slices. Three-dimensional (3D) images and projections from z-stack were constructed and processed using Leica Application Suite X software (LASX). Images were analyzed using LASX and FIJI software. The cell volume was calculated on EGFP-signal in each Z-stack using ImageJ Macro Code.

2.7 | Apoptosis assay by flow cytometry

For flow cytometry experiments, MCD4 and HK-2 cells were grown onto a six multiwell plate and treated with FTI-277 and Palmitic Acid (positive control) or transiently transfected. Briefly, cell apoptosis was assessed by Annexin-V-PE/7-AAD staining (Becton Dickinson) according to manufacturer's instructions. Samples were acquired for flow cytometry (FACScanto II; Becton Dickinson) and analyzed using FACS Diva software (Becton Dickinson). For transiently transfected cells, the percentage of apoptotic cells was assessed on gated EGFP⁺ cells.

2.8 | Statistical analysis

All values are reported as means ± SEM. Statistical analysis was performed by one-way analysis of variance (ANOVA) or two-way ANOVA, followed by Dunnett's or Tukey's multiple comparisons tests. When applicable, the Student t-test was also applied. A difference of $p < 0.05$ was considered statistically significant.

3 | RESULTS

3.1 | FTI-277 treatment decreases cell volume

Unlike the other Rho family proteins, RhoB can be either geranylgeranylated (RhoB-GG) or farnesylated (RhoB-F), representing the only

target for the FTI. Cell size was evaluated in cells resuspended either in an isosmotic solution containing NaCl (iso-NaCl 300 mOsm/L) or in an isotonic solution containing the impermeable solute, mannitol (M), instead of NaCl (iso-M 300 mOsm/L). Compared to untreated cells, treatment with FTI significantly reduced the cell size as assessed by using the electronic sizing LUNA (LUNA-II™ Automated Cell Counter) (Table 1). Similar results were obtained in HK-2 cells (Table S1). Moreover, cell size was also measured in hypertonic challenge (Table S2).

Changes in cell volume were further investigated by applying a fluorescent approach using calcein-AM. Notably, calcein exhibits a concentration-dependent quenching by proteins or salt, so changes in fluorescence signals are directly correlated to changes in cell volume. Briefly, MCD4 cells were loaded with calcein-AM (10 μM for 45 min). Cells were perfused either with iso-NaCl or with iso-M. Compared to untreated cells (Untreated), FTI-277 treatment (FTI) significantly reduced the fluorescence emission signal with both iso-NaCl or iso-M solutions (Table 1) following cell volume reduction. Similar observations were obtained in HK-2 cells (Table S1).

3.2 | FTI-277 treatment alters hyperosmotic-dependent cell shrinkage response

Hyperosmotic shrinkage results from exposure to a hypertonic external environment. Here, the shrinkage capability of cells, in the absence or the presence of FTI-277, was evaluated. To this end, cells were labeled with calcein-red orange and exposed to a hypertonic sodium chloride (NaCl) or mannitol (M) solution gradient (400 and 500 mOsm/L). As mentioned above, changes in the fluorescence emission signals were normalized against the cell area that correlated to the changes in cell volume. In untreated cells, the normalized fluorescence signal significantly decreased after exposure to both hyper-solutions (400 and 500 mOsm/L), (Figure 1). By contrast, in FTI-treated cells, a slight but not significant reduction in the normalized fluorescence signal was detected when cells were exposed to the first hyper-solution (400 mOsm/L). Conversely, compared to the basal condition, a significant decrease in the

TABLE 1 Cell volume measurement in MCD4 cells in the presence of isotonic NaCl or M solution.

Solution	Cell volume measurement method	Untreated	Farnesyltransferase inhibitor (FTI)
iso-NaCl 300 mOsm/L	Electronic cell sizing LUNA (μm)	9.49 ± 0.12 n = 21	8.79 ± 0.27 n = 17*
	Calcein-based fluorescence assay (a.u.)	100 ± 4.15 n = 159	76.48 ± 2.68 n = 147****
iso-M 300 mOsm/L	Electronic cell sizing LUNA (μm)	8.99 ± 0.11 n = 16	7.53 ± 0.38 n = 11***
	Calcein-based fluorescence assay (a.u.)	100 ± 3.88 n = 98	85.08 ± 4.74 n = 97*

Note: Values represent the mean ± SEM and analyzed by Student t-test (* $p < 0.05$, *** $p < 0.001$, and **** $p < 0.0001$ vs. untreated).

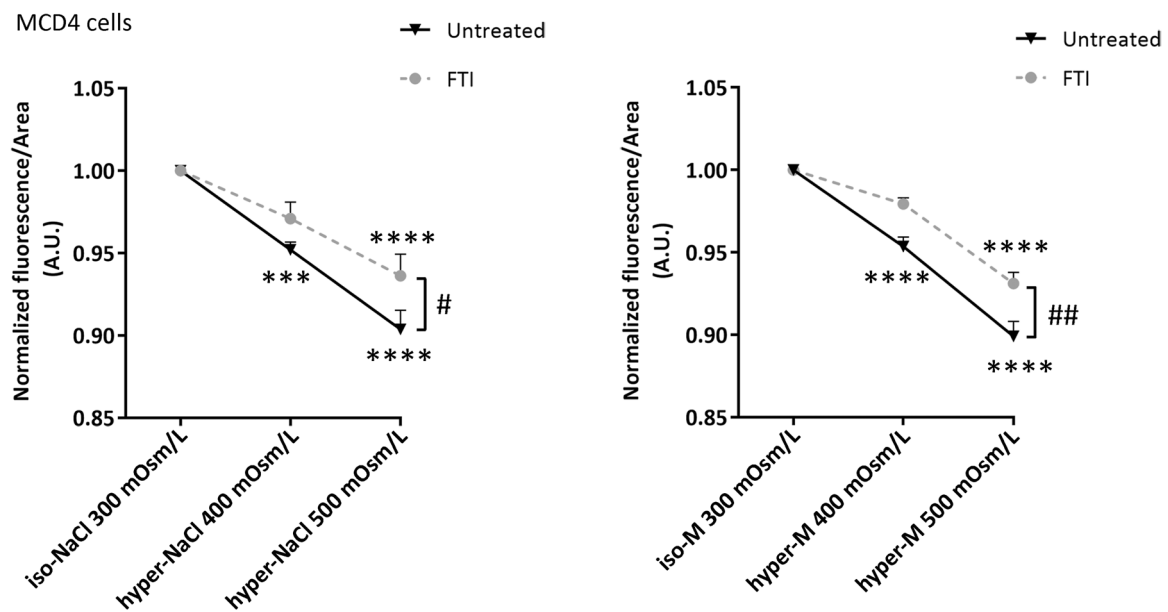


FIGURE 1 Evaluation of cell volume changes following exposure to the hypertonic (NaCl or M) solution gradient. MCD4 cells were left untreated or treated with FTI-277, as described in Section 2. Exposure of untreated cells to hypertonic sodium chloride (NaCl) or mannitol (M) solution gradient significantly reduced the fluorescence emission signal. Farnesyltransferase inhibitor (FTI)-treated cells did not respond to hyper 400 mOsm/L, but a significant reduction in the fluorescence was observed in the presence of hyper 500 mOsm/L. Values are expressed as means \pm SEM and analyzed by two-way analysis of variance followed by Dunnett's (** $p < 0.001$ and **** $p < 0.0001$ vs. iso 300 mOsm/L) and Sidak's Multiple Comparison test (# $p < 0.05$ and ## $p < 0.01$ vs. untreated).

normalized fluorescence signal was measured in cells exposed to the second hyper-solution (500 mOsm/L). Of note, this latter response is significantly different from that observed in untreated cells subjected to the same solution gradient. Similar results were obtained using both the NaCl and mannitol gradients (Figure 1). This impairment of the FTI-277 treated cells in responding to the hyper-solutions might be explained considering that FTI-277 treated cells are already partially shrunk, and therefore display a lower ability to respond to the hypertonic solution compared to untreated cells.

3.3 | Hyperosmolarity activates the small GTPase RhoB

In vitro studies revealed that hyperosmotic stress activates proteins of the Rho family (Di Ciano-Oliveira et al., 2003; Lunn & Rozengurt, 2004), which are pivotal players in controlling actin remodeling. Here, the selective activity of RhoB was evaluated using a specific FRET sensor (Reinhard et al., 2016) in renal collecting duct MCD4 cells, in the absence or the presence of FTI-277. Cells were first perfused with an isosmotic solution (iso-NaCl) and then exposed to a hyperosmotic sodium chloride solution gradient. Compared to the basal state, hyperosmotic solutions caused a rapid and significant increase in the FRET signal, consistent with increased RhoB activity. By contrast, no relevant changes in the FRET signal and therefore in RhoB activity were observed when cells were exposed to a hyposmolar NaCl solution (Figure 2a). RhoB activity was also evaluated using mannitol (M), an impermeable solute, instead of

NaCl. Similarly, hypertonicity significantly stimulated RhoB. No relevant changes were observed under hypotonicity (Figure 2b). Of note, RhoB activation, elicited by hyperosmotic (NaCl or M) solutions, was also observed in the presence of FTI-277 (Figure 3a,b). Similar results were obtained also in HK-2 cells (Figure S1), likely suggesting that RhoB can be considered a general sensor for hypertonicity and that FTI-277 treatment did not affect the activation of RhoB elicited by hyperosmolarity. Interestingly, semi-quantitative analysis of confocal fluorescence intensity revealed that treatment with hyperosmolar solutions significantly increased F-actin content (Table S3).

3.4 | Impairment of RhoB farnesylation alters the hyperosmotic-dependent cell shrinkage response

Besides RhoB, other small GTPases including H-Ras, Rheb, CENP-E, and CENP-F are targets of the FTIs (Pan & Yeung, 2005). Therefore, to better define the involvement of RhoB in modulating cell volume, the shrinkage capability was analyzed in cells encoding for RhoB-wt-EGFP and RhoB-CLLL-EGFP, a mutant that cannot undergo farnesylation (Gong et al., 2018). Interestingly, exposure of RhoB-wt-EGFP expressing cells to both hyper-solutions (400 and 500 mOsm/L) caused a significant reduction in the normalized fluorescence signal that correlates to a decrease in the cell volume (Figure 4). Similar findings were obtained in cells expressing EGFP as an internal control. By contrast, in cells expressing the RhoB-CLLL-EGFP a slight but not significant reduction in the normalized fluorescence signal was detected when cells were exposed to the

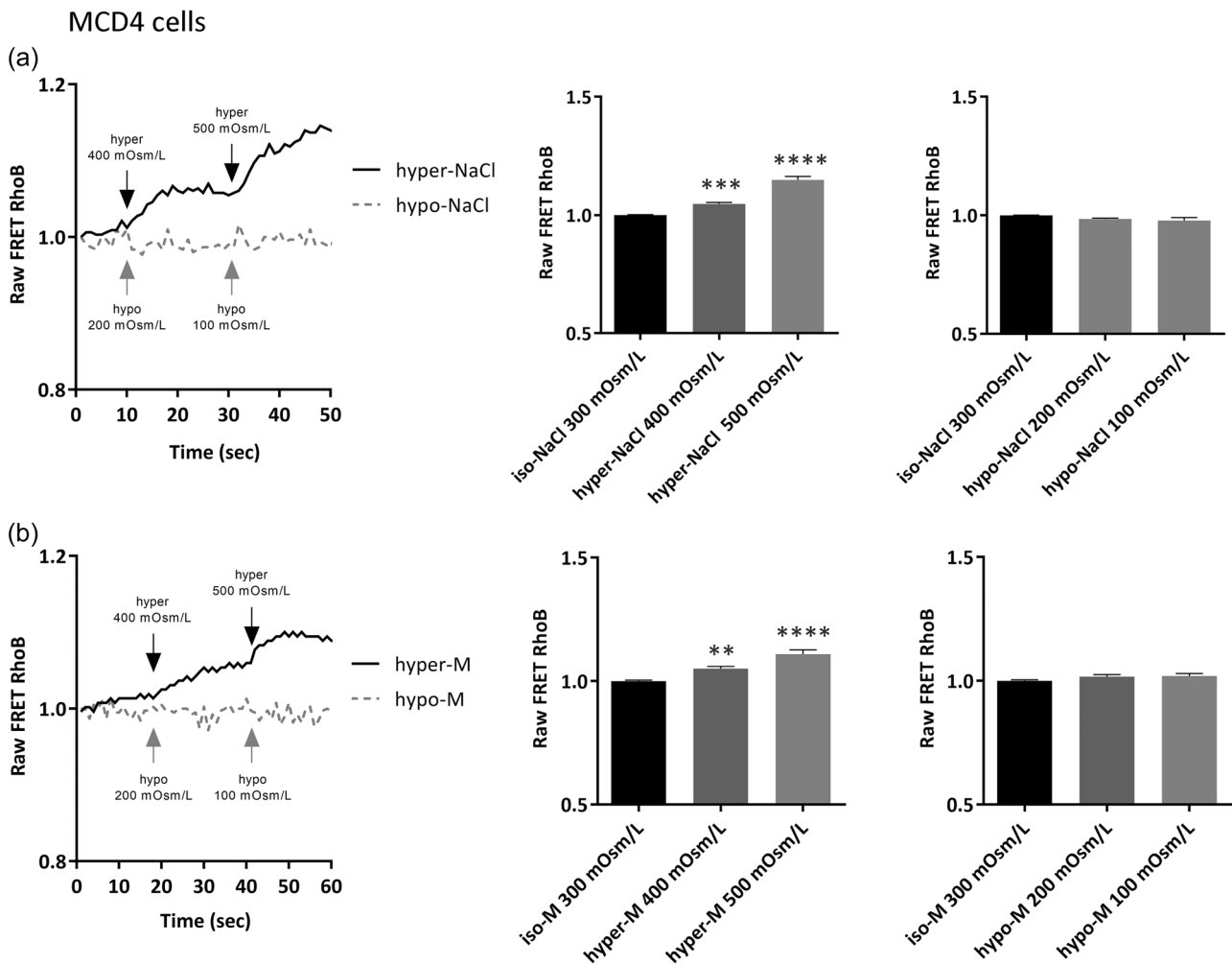


FIGURE 2 Effect of hyperosmotic stress on RhoB activity. MCD4 cells were transiently transfected with the RhoB-FRET sensor, as described in Section 2. On the left, a representative time course of the fluorescence resonance energy transfer (FRET) signal recorded at single cell level upon osmotic stress stimulation. On the right, a bar plot showing the mean \pm SEM values of the raw FRET. Note that exposure to hypertonic sodium chloride (a) or mannitol (b) solution gradient (400 and 500 mOsm/L) induced a significant increase of RhoB activity with respect to cells in isotonic solution (300 mOsm/L). No relevant changes were observed under hypotonic (NaCl or M) stress. Data are expressed as means \pm SEM and analyzed by one-way analysis of variance followed by Dunnett's Multiple Comparison test (** $p < 0.01$, *** $p < 0.001$ and **** $p < 0.0001$ vs. iso 300 mOsm/L).

first hyper-solution (400 mOsm/L). Instead, compared to the initial state condition, a significant reduction in the normalized fluorescence signal was measured only in cells exposed to the second hyper-solution (500 mOsm/L), (Figure 4). Of note, this latter response is significantly different from that observed in RhoB-wt-EGFP expressing cells. Similar results were obtained using both the NaCl and mannitol gradients. Also, RhoB-wt-EGFP and RhoB-CLLL-EGFP proteins displayed similar cellular localization (Figure S2).

3.5 | Inhibition of RhoB farnesylation is associated with a cell volume decrease

Renal collecting duct MCD4 cells were transfected as reported above. Confocal microscopy followed by 3D reconstruction and

quantitative analysis of cell volume using EGFP-signal in each X-Y plane was performed. 3D reconstruction, z-projections, and volume analysis revealed that compared to cells expressing RhoB-wt-EGFP, RhoB-CLLL-EGFP-expressing cells displayed a significant reduction in cell volume (Figure 5). Similar results were obtained in HK-2 cells (Figure 6). To test whether this reduction in cell volume could be related to the morphological rearrangements occurring during apoptosis, MCD4, and HK-2 cells were stained for Annexin V and 7-AAD and analyzed by flow cytometry. Treatment with Palmitic acid (250 μ M for 24 h at 37°C) was used as an internal positive control. Compared to untreated cells, FTI-277 treatment enhanced cell apoptosis by increasing the percentage values of both early and late apoptosis (Figure 7a). Analysis of cell apoptosis on gated EGFP⁺ transfected cells showed that the RhoB-CLLL-EGFP-expressing cells had a significant increase in cell apoptosis compared with the

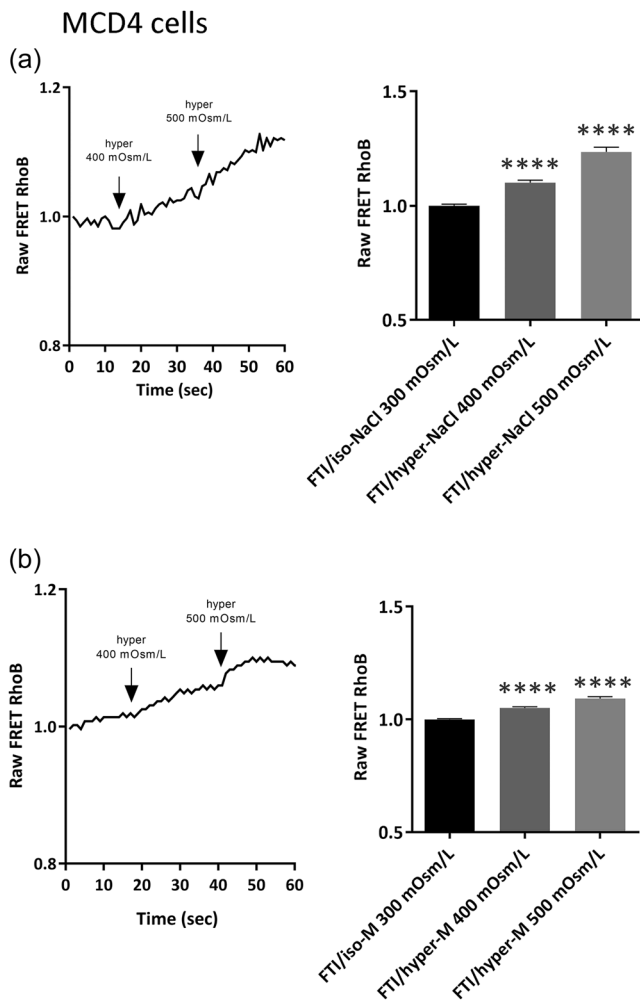


FIGURE 3 Effect of farnesyltransferase inhibitor (FTI) treatment on hyperosmotic RhoB activation. MCD4 cells were transiently transfected with the RhoB-fluorescence resonance energy transfer (FRET) sensor, as described in Section 2. On the left, a representative time course of the FRET signal recorded at single cell level upon osmotic stress stimulation. On the right, a bar plot showing the mean \pm SEM values of the Raw FRET. Note that RhoB activation under hypertonic sodium chloride (a) or mannitol (b) solution is also observed in the presence of FTI inhibitor. Data are expressed as means \pm SEM and analyzed by one-way analysis of variance followed by Dunnett's Multiple Comparison test (**** $p < 0.0001$ vs. iso 300 mOsm/L).

RhoB-wt-EGFP-expressing cells (Figure 7b). Similar results were observed in HK-2 cells treated with FTI-277 (Figure S3a) as well as in RhoB-CLLL-EGFP-expressing HK-2 cells (Figure S3b).

4 | DISCUSSION

Despite decades of research, how cells dynamically manage their volume is poorly understood. Changes in cell volume might originate from exposure to external aniso-osmotic solutions. Alternatively, ions or osmolytes transport across the plasma membrane, or

polymerization and depolymerization of molecules, affecting the intracellular osmotic force, can also alter cell volume (Di Ciano-Oliveira et al., 2006). Several studies propose that small GTP-binding proteins of the Rho family are part of the complex cellular machinery activated during exposure to aniso-osmotic solutions. The Rho family proteins include about 22 components (Di Ciano-Oliveira et al., 2006). These monomeric G-proteins can switch from the inactive GDP-bound to the active GTP-bound form, thereby modulating different signal transduction pathways. Mostly, Rho proteins play a paramount role in controlling the state of actin cytoskeleton polymerization. Numerous pieces of evidence revealed that cell shrinkage, induced by hyperosmolarity, is associated with a strong formation of actin filaments that accumulate at the peripheral membrane constituting an actin ring. Conversely, during hypotonicity, a significant decrease in ventral F-actin was detected in several cell lines (Tilly et al., 1996). In rat fibroblasts, hypotonicity promotes the formation of membrane protrusions through the activation of Cdc42 and Rac-1 (Carton et al., 2003). Hyperosmolarity also causes a strong activation of Rac-1 and Cdc42 (Lewis et al., 2002). These observations might be explained considering that cell swelling or shrinkage may both cause alteration in cell shape and volume possibly through selective tensile proteins. Nevertheless, whether other G-proteins participate in controlling these processes remains still elusive. Here, the involvement of the small GTPase RhoB in modulating the cellular responses to hyperosmolarity has been evaluated in two different renal cell models, the collecting duct MCD4 cells and the proximal tubule HK-2 cells. FRET studies revealed that RhoB is stimulated by hyperosmolarity but not by hyposmolarity making RhoB a molecular sensor only for hyperosmolarity. The Rho subfamily comprises structurally similar components RhoA, RhoB, and RhoC (Vega & Ridley, 2008). Despite their similarity, RhoB is the one that can be either farnesylated or geranylgeranylated whereas other Rho subfamily proteins can be only geranylgeranylated (Adamson et al., 1992). The biological function of RhoB is tightly modulated by its prenylation status (Mazières et al., 2005). In fact, only geranylgeranylated RhoB, and not the farnesylated, counteracts the Ras transformation of fibroblast (Mazières et al., 2005). Moreover, exposure to FTIs resulted in the loss of farnesylation paralleled by a gain of geranylgeranylated RhoB (Du & Lebowitz, & Prendergast, 1999; Lebowitz et al., 1997). Therefore, we might assume that changes in cell volume might be likely related to an increase of geranylgeranylated RhoB. FTIs were initially generated to block Ras, whose activity is dependent on its farnesylation status. Nevertheless, numerous studies showed that the anti-oncogenic features of FTIs were not associated with Ras inhibition but rather targeted the function of RhoB, which like Ras, and as already stated above, can be also farnesylated (Prendergast, 2001b). In the first instance, incubation with FTI-277 significantly reduced the cell size either in resuspended or adherent cells as assessed by using an Automated Cell Counter and a calcein-based imaging approach. In addition, compared to untreated cells, exposure to FTI-277 resulted in an abnormal response to hyperosmolarity as cells displayed a reduced shrinkage ability only at the highest concentrated gradient. This effect might be explained by

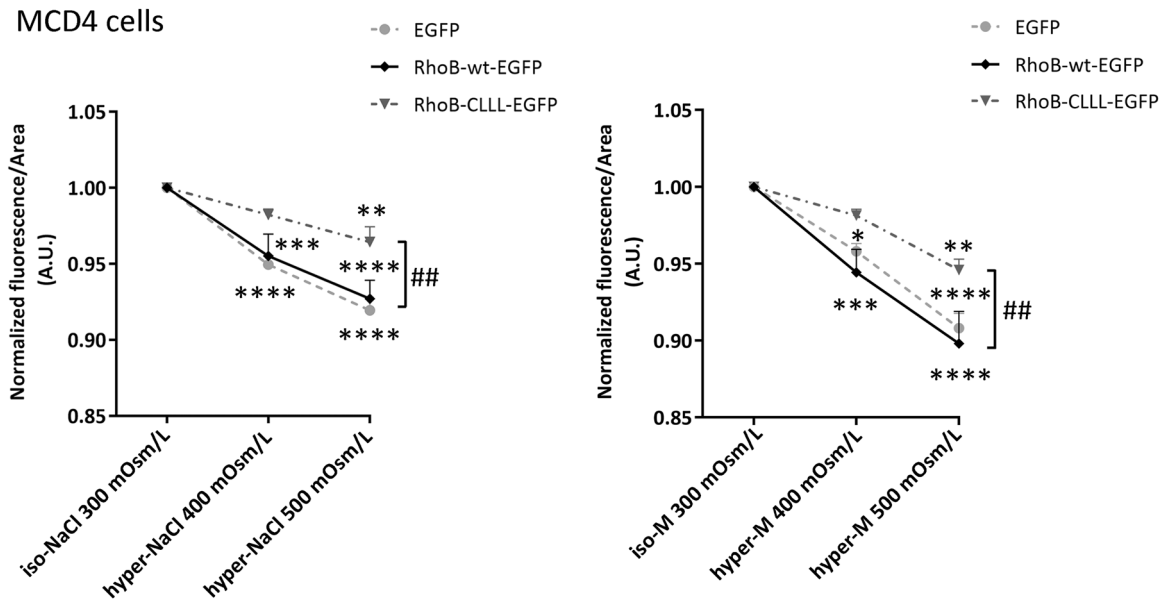


FIGURE 4 Evaluation of cell volume changes following exposure to the hypertonic (NaCl or M) solution gradient. MCD4 cells were transiently transfected with enhance green fluorescence protein (EGFP), RhoB-wt-EGFP, or RhoB-CLLL-EGFP, as described in Section 2. Exposure of RhoB-wt-EGFP or EGFP-expressing cells to hypertonic solution gradient caused a significant reduction in the fluorescence that correspond to a reduction in the cell volume. Cells expressing the RhoB-CLLL-EGFP mutant, did not respond to the solution of 400 mOsm/L, however, a significant reduction in the fluorescence was observed when RhoB CLLL-EGFP expressing cells were exposed to very high osmotic stresses 500 mOsm/L. Values are expressed as means \pm SEM and analyzed by two-way analysis of variance followed by Dunnett's ($*p < 0.05$, $**p < 0.01$, $***p < 0.001$ and $****p < 0.0001$ vs. iso 300 mOsm/L) and Sidak's multiple comparison test ($##p < 0.01$ vs. RhoB-wt-EGFP).

MCD4 cells

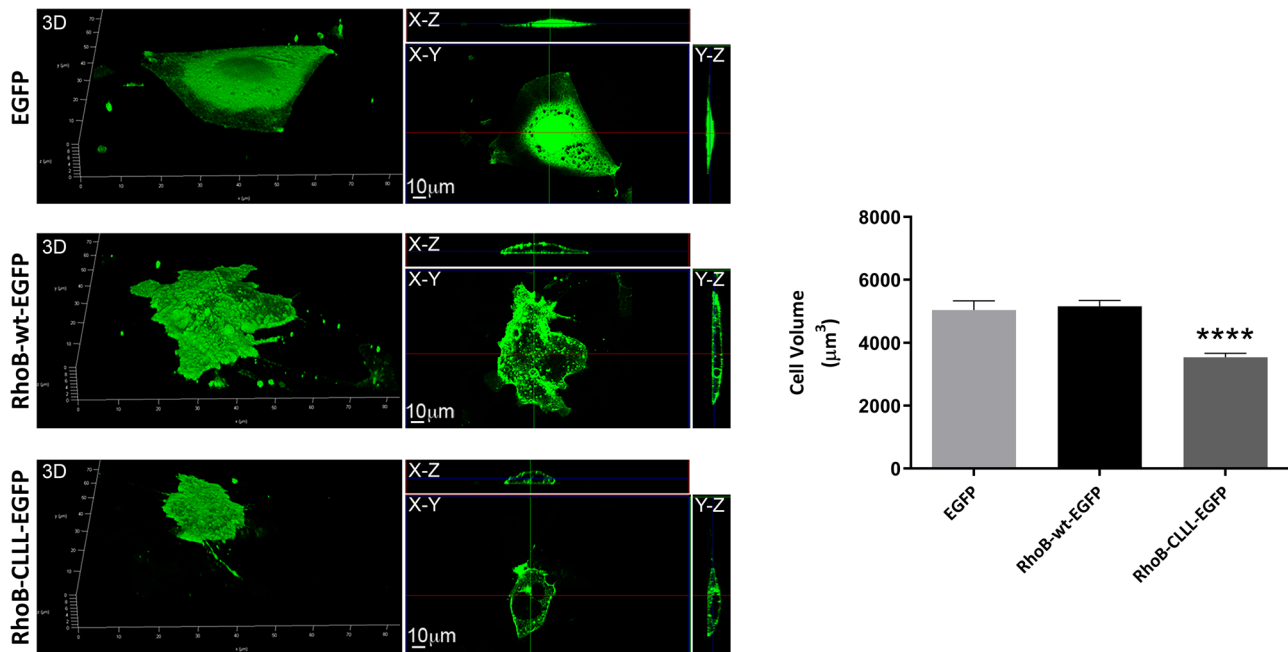


FIGURE 5 Confocal microscopy followed by 3D reconstruction, z-projections, and measure of cell volume using enhance green fluorescence protein (EGFP) signal in MCD4 cells after transfection with RhoB-wt-EGFP, RhoB-CLLL-EGFP, and empty vector (EGFP). On the left, 3D reconstructions, x-y planes and z-projections of EGFP-tagged protein transfected in MCD4 cells as described in Section 2. Scale bar, 10 μ m. On the right, a bar plot showing the cell volume (μm^3) of the transfected cells. Values are expressed as means \pm SEM and analyzed by one-way analysis of variance followed by Dunnett's Multiple Comparison test ($****p < 0.0001$ vs. EGFP).

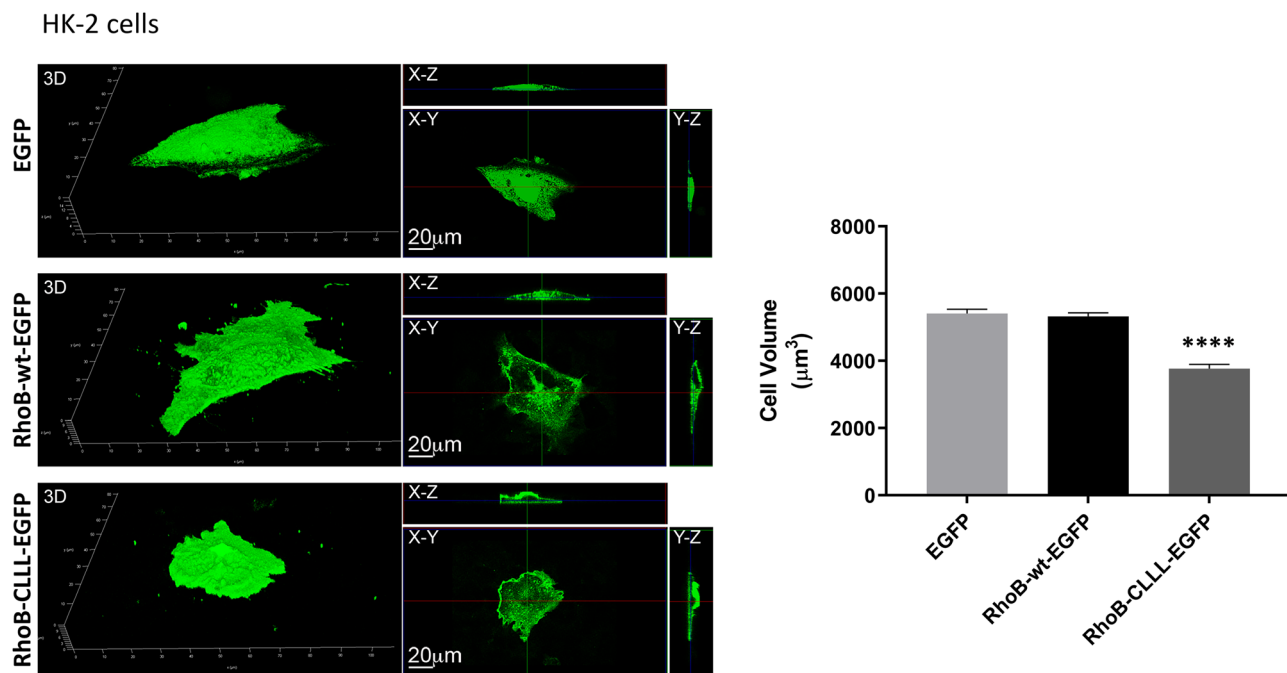


FIGURE 6 Confocal analysis and 3D reconstruction of cell volume in HK-2 cells after transfection with RhoB-wt-enhance green fluorescence protein (EGFP), RhoB-CLLL-EGFP, and empty vector (EGFP). On the left, 3D reconstruction of a confocal z-stack of EGFP-tagged protein transfected in HK-2 cells. Scale bar, 20 μm. On the right, a bar plot showing the values of the quantification of cell volume of the cells transfected as indicated. Values are expressed as means ± SEM and analyzed by one-way analysis of variance followed by Dunnett's Multiple Comparison test (**** $p < 0.0001$ vs. EGFP).

MCD4 cells

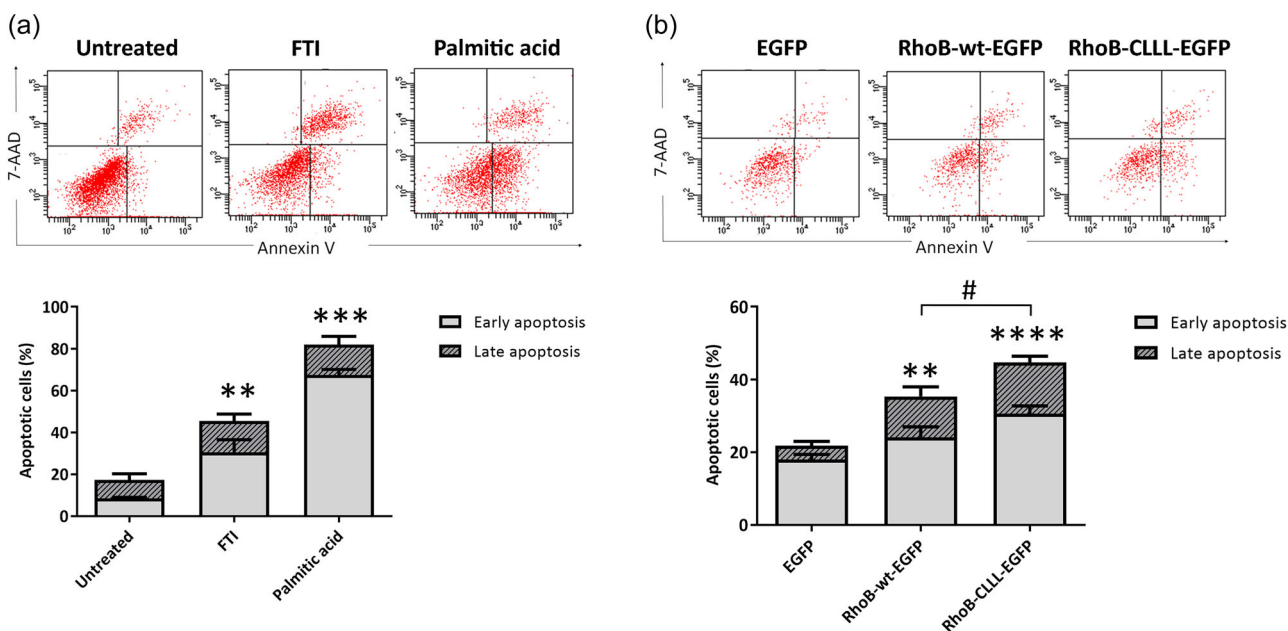


FIGURE 7 Effect of inhibition of RhoB farnesylation on apoptosis in MCD4 cells. (a) MCD4 cells were treated with FTI-277 or Palmitic Acid (positive control) and analyzed for cell apoptosis by Annexin-V-PE/7-AAD staining. At the top, a representative dot plot analysis is shown. At the bottom, the bar graph shows the percentage values of early and late apoptotic cells. Values are expressed as means ± SEM and analyzed by one-way analysis of variance (ANOVA) followed by Dunnett's multiple comparison test (** $p < 0.01$ and *** $p < 0.001$ vs. untreated). (b) MCD4 cells were transfected with EGFP (empty vector), RhoB-wt-EGFP, or RhoB-CLLL-EGFP and the percentage of cell apoptosis was assessed by Annexin-V-PE/7-AAD staining on gated EGFP⁺ cells. At the top, a representative dot plot analysis is shown. At the bottom, the bar graph shows the percentage values of early and late apoptotic cells. Values are expressed as means ± SEM and analyzed by one-way ANOVA followed by Tukey's multiple comparison test (** $p < 0.01$ and **** $p < 0.0001$ vs. EGFP; # $p < 0.05$ vs. RhoB-wt-EGFP).

considering that FTI-277 treated cells are already partially shrunk to a steady state. Therefore, compared to untreated cells, the FTI-dependent cell size reduction might interfere with the shrinkage ability of the cell membrane. Furthermore, to exclude that the volume change response could be related to altered membrane potential, due to NaCl itself, measurements were performed using a mannitol-based osmotic gradient (Mola et al., 2016). Data showed that similar volume changes were detected either using a NaCl gradient or a mannitol-based gradient, likely suggesting that the observed changes in cell size are related to the level of membrane shrinkage. Similar results were obtained in both renal cell models, the collecting duct MCD4 cells and the proximal HK-2 likely indicating that the FTI-277-induced cell volume changes occurred through a general cellular mechanism independently of the cell type in the renal tubule.

Farnesylation is a lipid modification occurring on the cysteine residue of the CAAX-box that is commonly shared with several intracellular proteins including numerous G proteins, intracellular and nuclear surface membrane proteins (Gao et al., 2009). Therefore, to recognize the role of RhoB in sensing hyperosmolarity, the volume change ability was analyzed in cells expressing the RhoB-wt-EGFP and RhoB-CLLL-EGFP, a mutant that cannot undergo farnesylation (Gong et al., 2018). RhoB-wt-EGFP expressing cells responded to both NaCl and mannitol gradients in terms of reduction in calcein fluorescence, which is related to cell shrinkage. Therefore, the expression of the RhoB wild type would not affect the ability to respond to hyperosmolarity. By contrast and like what was observed in FTI-277 treated cells, calcein fluorescence reduction was significant only in RhoB-CLLL-EGFP cells perfused with the solution having the highest NaCl or mannitol gradient (500 mOsm/L). These findings strongly support the hypothesis that, among several intracellular proteins, FTI-277 targets RhoB also in renal cells. Moreover, it is well established that the apoptotic response to FTIs is mediated by RhoB (Vega & Ridley, 2018). Notably, volume loss is a typical feature of cell apoptosis (Benson et al., 1996). In this respect, it is crucial to underline that RhoB plays a key role in promoting the apoptosis process in cancer cells (Chen et al., 2000; Chung et al., 2013; Kim et al., 2010, 2011). Accordingly, flow cytometry experiments revealed that treatment with FTI-277 significantly increased apoptosis both in MCD4 as well as in HK-2 cells. In addition, it has also been found that RhoB-CLLL-EGFP mutants enhance the ability of MCD4 and HK-2 cells to proceed toward apoptosis (early or late apoptosis) compared to EGFP and RhoB-wt-EGFP transfected cells. This observation might explain the reason why RhoB-CLLL-EGFP mutant cells displayed a reduced cell volume at a steady state compared to EGFP and RhoB-wt-EGFP. Thus, impairment of RhoB farnesylation causes a decrease in cell size enhancing the ability of cells to proceed toward apoptosis.

5 | CONCLUSIONS

These data propose (i) RhoB as a molecular sensor for hyperosmolarity and not hyposmolarity; (ii) preventing RhoB farnesylation facilitates cell apoptosis, likely suggesting that RhoB might be considered a key protein playing a role in modulating cell apoptosis

by interfering with signals involved in the control of cell volume changes. To conclude these findings might have an important clinical impact as proposing RhoB farnesylation as a therapeutic target to promote cell apoptosis by modulating cell volume changes also in response to hyperosmolarity. By providing an insight into the involvement of RhoB farnesylation on cell size regulation, this study will support future research investigations addressing the interplay between small GTPases, cell remodeling, and apoptosis in health and disease.

AUTHOR CONTRIBUTIONS

Grazia Tamma, Ilaria Saltarella, and Mariangela Centrone conceived and supervised the study. Mariangela Centrone, Ilaria Saltarella, and Marianna Ranieri designed experiments. Mariangela Centrone, Ilaria Saltarella, Mariagrazia D'Agostino and Francesco Pisani performed experiments. Maria Venneri, Annarita Di Mise, and Laura Simone provided new tools and reagents. Grazia Tamma and Giovanna Valenti analyzed data. Mariangela Centrone, Ilaria Saltarella, Maria Antonia Frasanito, and Grazia Tamma wrote the manuscript.

ACKNOWLEDGMENTS

This work was supported by a project PRIN (2017R5ZE2C_002) to Grazia Tamma.

CONFLICT OF INTEREST STATEMENT

The authors declare no conflict of interest.

ORCID

Grazia Tamma  <http://orcid.org/0000-0002-8890-0278>

REFERENCES

- Adamson, P., Marshall, C. J., Hall, A., & Tilbrook, P. A. (1992). Post-translational modifications of p21rho proteins. *Journal of Biological Chemistry*, 267(28), 20033–20038.
- Arrazola Sastre, A., Luque Montoro, M., Gálvez-Martín, P., Lacerda, H. M., Lucia, A., Llaveró, F., & Zugaza, J. L. (2020). Small GTPases of the Ras and Rho families switch on/off signaling pathways in neurodegenerative diseases. *International Journal of Molecular Sciences*, 21(17), 6312. <https://doi.org/10.3390/ijms21176312>
- Benson, R. S., Heer, S., Dive, C., & Watson, A. J. (1996). Characterization of cell volume loss in CEM-C7A cells during dexamethasone-induced apoptosis. *American Journal of Physiology-Cell Physiology*, 270(4 Pt 1), C1190–C1203. <https://doi.org/10.1152/ajpcell.1996.270.4.C1190>
- Carton, I., Hermans, D., & Eggermont, J. (2003). Hypotonicity induces membrane protrusions and actin remodeling via activation of small GTPases Rac and Cdc42 in Rat-1 fibroblasts. *American Journal of Physiology-Cell Physiology*, 285(4), C935–C944. <https://doi.org/10.1152/ajpcell.00069.2003>
- Centrone, M., D'Agostino, M., Ranieri, M., Mola, M. G., Faviana, P., Lippolis, P. V., Silvestris, D. A., Venneri, M., Di Mise, A., Valenti, G., & Tamma, G. (2022). dDAVP downregulates the AQP3-mediated glycerol transport via V1aR in human colon HCT8 cells. *Frontiers in Cell and Developmental Biology*, 10, 919438. <https://doi.org/10.3389/fcell.2022.919438>
- Chaouhan, H. S., Vinod, C., Mahapatra, N., Yu, S. H., Wang, I. K., Chen, K. B., Yu, T. M., & Li, C. Y. (2022). Necroptosis: A pathogenic negotiator in human diseases. *International Journal of Molecular Sciences*, 23(21), 12714. <https://doi.org/10.3390/ijms232112714>

- Chen, Z., Sun, J., Pradines, A., Favre, G., Adnane, J., & Sebti, M. (2000). Both farnesylated and geranylgeranylated RhoB inhibit malignant transformation and suppress human tumor growth in nude mice. *Journal of Biological Chemistry*, 275(24), 17974–17978. <https://doi.org/10.1074/jbc.C000145200>
- Chung, K. S., Han, G., Kim, B. K., Kim, H. M., Yang, J. S., Ahn, J., Lee, K., Song, K. B., & Won, M. (2013). A novel antitumor piperazine alkyl compound causes apoptosis by inducing RhoB expression via ROS-mediated c-Abl/p38 MAPK signaling. *Cancer Chemotherapy and Pharmacology*, 72(6), 1315–1324. <https://doi.org/10.1007/s00280-013-2310-y>
- Ciano-Oliveira, C. D., Sirokmány, G., Szászi, K., Arthur, W. T., Masszi, A., Peterson, M., Rotstein, O. D., & Kapus, A. (2003). Hyperosmotic stress activates Rho: Differential involvement in Rho kinase-dependent MLC phosphorylation and NKCC activation. *American Journal of Physiology-Cell Physiology*, 285(3), C555–C566. <https://doi.org/10.1152/ajpcell.00086.2003>
- Di Ciano-Oliveira, C., Thirone, A. C. P., Szászi, K., & Kapus, A. (2006). Osmotic stress and the cytoskeleton: The R(h)ole of Rho GTPases. *Acta Physiologica*, 187(1–2), 257–272. <https://doi.org/10.1111/j.1748-1716.2006.01535.x>
- Du, W., Lebowitz, P. F., & Prendergast, G. C. (1999). Cell growth inhibition by farnesyltransferase inhibitors is mediated by gain of geranylgeranylated RhoB. *Molecular and Cellular Biology*, 19(3), 1831–1840. <https://doi.org/10.1128/mcb.19.3.1831>
- Du, W., & Prendergast, G. C. (1999). Geranylgeranylated RhoB mediates suppression of human tumor cell growth by farnesyltransferase inhibitors. *Cancer Research*, 59(21), 5492–5496.
- Economidou, D., Stavrinou, E., Giamalis, P., Dimitriadis, C., Economou, S., & Memmos, D. (2011). Acute kidney injury due to osmotic nephrosis following intraoperative placement of an intraperitoneal antiadhesive barrier. *American Journal of Kidney Diseases*, 57(2), 304–307. <https://doi.org/10.1053/j.ajkd.2010.10.044>
- Erickson, G. R., Northrup, D. L., & Guilak, F. (2003). Hypo-osmotic stress induces calcium-dependent actin reorganization in articular chondrocytes. *Osteoarthritis and Cartilage*, 11(3), 187–197. [https://doi.org/10.1053/s1063-4584\(02\)00347-3](https://doi.org/10.1053/s1063-4584(02)00347-3)
- Gao, J., Liao, J., & Yang, G. Y. (2009). CAAX-box protein, prenylation process and carcinogenesis. *American Journal of Translational Research*, 1(3), 312–325.
- Gong, X., Didan, Y., Lock, J. G., & Strömblad, S. (2018). KIF13A-regulated RhoB plasma membrane localization governs membrane blebbing and blebby amoeboid cell migration. *The EMBO Journal*, 37(17), e98994. <https://doi.org/10.15252/emboj.201898994>
- Henn, V., Edemir, B., Stefan, E., Wiesner, B., Lorenz, D., Theilig, F., Schmitt, R., Vossebein, L., Tamma, G., Beyermann, M., Krause, E., Herberg, F. W., Valenti, G., Bachmann, S., Rosenthal, W., & Klussmann, E. (2004). Identification of a novel A-kinase anchoring protein 18 isoform and evidence for its role in the vasopressin-induced aquaporin-2 shuttle in renal principal cells. *Journal of Biological Chemistry*, 279(25), 26654–26665. <https://doi.org/10.1074/jbc.M312835200>
- Iolascon, A., Aglio, V., Tamma, G., D'Apolito, M., Addabbo, F., Procino, G., Simonetti, M. C., Montini, G., Gesualdo, L., Debler, E. W., Svelto, M., & Valenti, G. (2007). Characterization of two novel missense mutations in the AQP2 Gene causing nephrogenic diabetes insipidus. *Nephron. Physiology*, 105(3), p33–p41. <https://doi.org/10.1159/000098136>
- Ju, J., & Gilkes, D. (2018). RhoB: Team oncogene or team tumor suppressor? *Genes*, 9(2), 67. <https://doi.org/10.3390/genes9020067>
- Kim, B. K., Kim, H. M., Chung, K. S., Kim, D. M., Park, S. K., Song, A., Won, K. J., Lee, K., Oh, Y. K., Lee, K., Song, K. B., Simon, J. A., Han, G., & Won, M. (2011). Upregulation of RhoB via c-jun N-terminal kinase signaling induces apoptosis of the human gastric carcinoma NUGC-3 cells treated with NSC12618. *Carcinogenesis*, 32(3), 254–261. <https://doi.org/10.1093/carcin/bgq244>
- Kim, C. H., Won, M., Choi, C. H., Ahn, J., Kim, B. K., Song, K. B., Kang, C. M., & Chung, K. S. (2010). Increase of RhoB in γ -radiation-induced apoptosis is regulated by c-jun N-terminal kinase in Jurkat T cells. *Biochemical and Biophysical Research Communications*, 391(2), 1182–1186. <https://doi.org/10.1016/j.bbrc.2009.12.012>
- Kitchen, P., Salman, M. M., Abir-Awan, M., Al-Jubair, T., Törnroth-Horsefield, S., Conner, A. C., & Bill, R. M. (2020). Calcein fluorescence quenching to measure plasma membrane water flux in live mammalian cells. *STAR Protocols*, 1(3), 100157. <https://doi.org/10.1016/j.xpro.2020.100157>
- Kültz, D. (2004). Hyperosmolality triggers oxidative damage in kidney cells. *Proceedings of the National Academy of Sciences United States of America*, 101(25), 9177–9178. <https://doi.org/10.1073/pnas.0403241101>
- Lebowitz, P. F., Casey, P. J., Prendergast, G. C., & Thissen, J. A. (1997). Farnesyltransferase inhibitors alter the prenylation and growth-stimulating function of RhoB. *Journal of Biological Chemistry*, 272(25), 15591–15594. <https://doi.org/10.1074/jbc.272.25.15591>
- Lewis, A., Di Ciano, C., Rotstein, O. D., & Kapus, A. (2002). Osmotic stress activates Rac and Cdc42 in neutrophils: Role in hypertonicity-induced actin polymerization. *American Journal of Physiology-Cell Physiology*, 282(2), C271–C279. <https://doi.org/10.1152/ajpcell.00427.2001>
- Liu, A., Cerniglia, G. J., Bernhard, E. J., & Prendergast, G. C. (2001). RhoB is required to mediate apoptosis in neoplastically transformed cells after DNA damage. *Proceedings of the National Academy of Sciences United States of America*, 98(11), 6192–6197. <https://doi.org/10.1073/pnas.111137198>
- Liu, Y., Belkina, N. V., Park, C., Nambiar, R., Loughhead, S. M., Patino-Lopez, G., Ben-Aissa, K., Hao, J. J., Kruhlak, M. J., Qi, H., von Andrian, U. H., Kehrl, J. H., Tyska, M. J., & Shaw, S. (2012). Constitutively active ezrin increases membrane tension, slows migration, and impedes endothelial transmigration of lymphocytes in vivo in mice. *Blood*, 119(2), 445–453. <https://doi.org/10.1182/blood-2011-07-368860>
- Lunn, J. A., & Rozengurt, E. (2004). Hyperosmotic stress induces rapid focal adhesion kinase phosphorylation at tyrosines 397 and 577. *Journal of Biological Chemistry*, 279(43), 45266–45278. <https://doi.org/10.1074/jbc.M314132200>
- Maeno, E., Ishizaki, Y., Kanaseki, T., Hazama, A., & Okada, Y. (2000). Normotonic cell shrinkage because of disordered volume regulation is an early prerequisite to apoptosis. *Proceedings of the National Academy of Sciences United States of America*, 97(17), 9487–9492. <https://doi.org/10.1073/pnas.140216197>
- Mazières, J., Tillement, V., Allal, C., Clanet, C., Bobin, L., Chen, Z., Sebti, S. M., Favre, G., & Pradines, A. (2005). Geranylgeranylated, but not farnesylated, RhoB suppresses Ras transformation of NIH-3T3 cells. *Experimental Cell Research*, 304(2), 354–364. <https://doi.org/10.1016/j.yexcr.2004.10.019>
- Mola, M. G., Sparaneo, A., Gargano, C. D., Spray, D. C., Svelto, M., Frigeri, A., Scemes, E., & Nicchia, G. P. (2016). The speed of swelling kinetics modulates cell volume regulation and calcium signaling in astrocytes: A different point of view on the role of aquaporins. *GLIA*, 64(1), 139–154. <https://doi.org/10.1002/glia.22921>
- Okada, Y., Maeno, E., Shimizu, T., Dezaki, K., Wang, J., & Morishima, S. (2001). Receptor-mediated control of regulatory volume decrease (RVD) and apoptotic volume decrease (AVD). *The Journal of Physiology*, 532(Pt 1), 3–16. <https://doi.org/10.1111/j.1469-7793.2001.0003g.x>
- Pan, J., & Yeung, S. C. J. (2005). Recent advances in understanding the antineoplastic mechanisms of farnesyltransferase inhibitors. *Cancer Research*, 65(20), 9109–9112. <https://doi.org/10.1158/0008-5472.Can-05-2635>

- Prendergast, G. C. (2001a). Actin' up: RhoB in cancer and apoptosis. *Nature Reviews Cancer*, 1(2), 162–168. <https://doi.org/10.1038/35101096>
- Prendergast, G. C. (2001b). Farnesyltransferase inhibitors define a role for RhoB in controlling neoplastic pathophysiology. *Histology and Histopathology*, 16(1), 269–275. <https://doi.org/10.14670/hh-16.269>
- Rasmussen, M., Alexander, R. T., Darborg, B. V., Møbjerg, N., Hoffmann, E. K., Kapus, A., & Pedersen, S. F. (2008). Osmotic cell shrinkage activates ezrin/radixin/moesin (ERM) proteins: Activation mechanisms and physiological implications. *American Journal of Physiology Cell Physiology*, 294(1), C197–C212. <https://doi.org/10.1152/ajpcell.00268.2007>
- Reinhard, N. R., van Helden, S. F., Anthony, E. C., Yin, T., Wu, Y. I., Goedhart, J., Gadella, T. W. J., & Hordijk, P. L. (2016). Spatiotemporal analysis of RhoA/B/C activation in primary human endothelial cells. *Scientific Reports*, 6, 25502. <https://doi.org/10.1038/srep25502>
- Sardini, A., Amey, J. S., Weylandt, K. H., Nobles, M., Valverde, M. A., & Higgins, C. F. (2003). Cell volume regulation and swelling-activated chloride channels. *Biochimica et Biophysica Acta (BBA) - Biomembranes*, 1618(2), 153–162. <https://doi.org/10.1016/j.bbamem.2003.10.008>
- Svetlitsyna, N., Semenova, N., & Tuchin, V. V. (2024). Conditions of acceleration and deceleration of the cancer cell growth under osmotic pressure. *Chaos: An Interdisciplinary Journal of Nonlinear Science*, 34(2). <https://doi.org/10.1063/5.0189550>
- Tamma, G., Procino, G., Strafino, A., Bononi, E., Meyer, G., Paulmichl, M., Formoso, V., Svelto, M., & Valenti, G. (2007). Hypotonicity induces aquaporin-2 internalization and cytosol-to-membrane translocation of ICln in renal cells. *Endocrinology*, 148(3), 1118–1130. <https://doi.org/10.1210/en.2006-1277>
- Tamma, G., Procino, G., Svelto, M., & Valenti, G. (2007). Hypotonicity causes actin reorganization and recruitment of the actin-binding ERM protein moesin in membrane protrusions in collecting duct principal cells. *American Journal of Physiology-Cell Physiology*, 292(4), C1476–C1484. <https://doi.org/10.1152/ajpcell.00375.2006>
- Thirone, A. C. P., Speight, P., Zulys, M., Rotstein, O. D., Szász, K., Pedersen, S. F., & Kapus, A. (2009). Hyperosmotic stress induces Rho/Rho kinase/LIM kinase-mediated cofilin phosphorylation in tubular cells: Key role in the osmotically triggered F-actin response. *American Journal of Physiology-Cell Physiology*, 296(3), C463–C475. <https://doi.org/10.1152/ajpcell.00467.2008>
- Tilly, B. C., Edixhoven, M. J., Tertoolen, L. G., Morii, N., Saitoh, Y., Narumiya, S., & de Jonge, H. R. (1996). Activation of the osmosensitive chloride conductance involves P21rho and is accompanied by a transient reorganization of the F-actin cytoskeleton. *Molecular Biology of the Cell*, 7(9), 1419–1427. <https://doi.org/10.1091/mbc.7.9.1419>
- Vega, F. M., & Ridley, A. J. (2008). Rho GTPases in cancer cell biology. *FEBS Letters*, 582(14), 2093–2101. <https://doi.org/10.1016/j.febslet.2008.04.039>
- Vega, F. M., & Ridley, A. J. (2018). The RhoB small GTPase in physiology and disease. *Small GTPases*, 9(5), 384–393. <https://doi.org/10.1080/21541248.2016.1253528>
- Venkova, L., Vishen, A. S., Lembo, S., Srivastava, N., Duchamp, B., Ruppel, A., Williard, A., Vassilopoulos, S., Deslys, A., Garcia Arcos, J. M., Diz-Muñoz, A., Balland, M., Joanny, J. F., Cuvelier, D., Sens, P., & Piel, M. (2022). A mechano-osmotic feedback couples cell volume to the rate of cell deformation. *eLife*, 11, 11. <https://doi.org/10.7554/eLife.72381>
- Wherlock, M., Gampel, A., Futter, C., & Mellor, H. (2004). Farnesyltransferase inhibitors disrupt EGF receptor traffic through modulation of the RhoB GTPase. *Journal of Cell Science*, 117(Pt 15), 3221–3231. <https://doi.org/10.1242/jcs.01193>
- Yue, J., & López, J. M. (2020). Understanding MAPK signaling pathways in apoptosis. *International Journal of Molecular Sciences*, 21(7), 2346. <https://doi.org/10.3390/ijms21072346>

SUPPORTING INFORMATION

Additional supporting information can be found online in the Supporting Information section at the end of this article.

How to cite this article: Centrone, M., Saltarella, I., D'Agostino, M., Ranieri, M., Venneri, M., Di Mise, A., Simone, L., Pisani, F., Valenti, G., Frassanito, M. A., & Tamma, G. (2024). RhoB plays a central role in hyperosmolarity-induced cell shrinkage in renal cells. *Journal of Cellular Physiology*, 1–12. <https://doi.org/10.1002/jcp.31343>